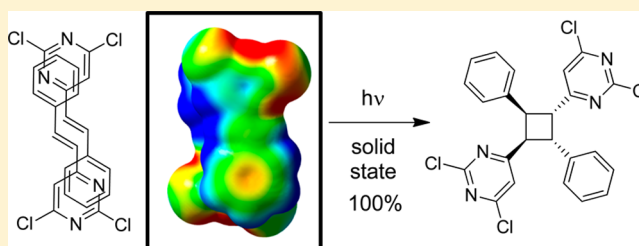


π - π Interaction Energies as Determinants of the Photodimerization of Mono-, Di-, and Triazastilbenes

Alexander A. Parent,[†] Daniel H. Ess,[‡] and John A. Katzenellenbogen^{*,†}[†]Department of Chemistry University of Illinois at Urbana-Champaign Urbana, Illinois 61801, United States[‡]Department of Chemistry and Biochemistry Brigham Young University Provo, Utah 84602, United States**S** Supporting Information

ABSTRACT: We describe the quantitative [2 + 2] photocycloaddition of crystalline *trans*-2,4-dichloro-6-styrylpyrimidine to produce the corresponding *htt r-ctt* cyclobutane dimer, and we present ¹H NMR analysis of the photolysis of this and six other mono-, di-, and triazastilbenes in solid and solution states. Density functional (M06-2X) and correlated ab initio (MP2) calculations were used to obtain interaction energies between two monomers of each azastilbene. These energies mirror the relative polarization of the stilbene moieties and can be quantitatively correlated with the rate of reaction and selective formation of the *htt r-ctt* dimers. In the solid state, poor correlation is observed between interaction energy and reactivity/selectivity. This lack of correlation is explained through X-ray analysis of the azastilbene monomers and is shown to be in accordance with the principles of Schmidt's topochemical postulate. Conversely, in solution there is a strong positive correlation ($R^2 = 0.96$) between interaction energies and formation of the *htt r-ctt* dimer. These results are the first to show this correlation and to demonstrate the utility of calculated interaction energies as a tool for the prediction of stereo- and regioselectivity in solution-state stilbene-type photocycloadditions.

**■ INTRODUCTION**

Although alkene photodimerization in the solid state, which holds the allure of controlling both regio- and stereochemistry on the basis of the crystal orientation of the reactants, has been known since the beginning of organic chemistry,¹ it has recently undergone a resurgence of interest due to applications in organic materials chemistry. While isolated reports from more than a century ago describe the regio- and stereoselectivity of this transformation,^{2–7} it was not until the 1960s that Schmidt articulated the “topochemical postulate”,⁸ which attempts to predict which alkenes readily undergo [2 + 2] photocycloaddition on the basis of the crystal packing of the starting alkenes.^{9–11} Schmidt noted two essential criteria for dimerization to occur: the double bonds of crystalline reactants must be parallel to each other, and the center-to-center distance of the reacting alkenes must be less than 4.2 Å apart. When these criteria are satisfied, photocycloaddition was predicted to proceed under “topochemical” control, producing selectively the regio- and stereoisomer dictated by the molecular packing of the alkenes in the crystal.

While Schmidt's principles successfully rationalized topochemical control in the solid-state photodimerization of cinnamic acids and many other disubstituted olefins, a range of exceptions to these rules developed, including crystalline olefins that failed to react as expected and crystals that underwent dimerization despite a lack of double-bond planarity or greatly increased separation of the reacting atoms. The “reaction cavity” concept, in which the inter- and intramolecular motion of the reactive pair is constrained by its crystal lattice,

was proposed by Cohen,¹² and this concept, together with crystal lattice energy calculations, effectively explained both positive and negative exceptions. For close-stacking, parallel-oriented disubstituted olefins with a <4.2 Å center-to-center distance that failed to react in the solid state, the lattice perturbation needed to accommodate the photodimerization product would have required an enormous input of energy (i.e., thousands of kcal/mol).¹³ Conversely, for alkenes that undergo dimerization yet had crystal packing predicted to be unreactive, calculations showed surprisingly little disturbance in their molecular environment despite the movement required for cyclobutane formation with minimal increase in lattice energy.^{14–16} Thus, while Schmidt's original topochemical postulate continues to be a good rule of thumb, additional exceptions that will doubtless arise will require a more in-depth analysis than a cursory examination of the X-ray crystal structure of the starting material. For excellent reviews, see Natarajan and Ramamurthy.^{17,18}

While the photochemistry of stilbenes and its derivatives has been well studied,^{17,19–24} there have been relatively few reports on the photolysis of stilbene derivatives with nitrogen-bearing rings. Nonetheless, the [2 + 2] photocycloaddition of 2- and 4-azastilbene derivatives has been studied extensively in both the solid and solution state. In solution, styrylpyridines, both as free bases and as various pyridinium salts, produce low yields of dimers upon irradiation, with the ionic compounds generally

Received: February 28, 2014

Published: May 16, 2014

giving higher cyclobutane yields and increased stereo- and regioselectivity.^{25–28} With 4-styrylpyridines, salt formation accelerated solution-state [2 + 2] photocycloaddition,²⁹ with increasing addition of acid giving more rapid and more selective dimer formation. In addition, when the highly polarized 4-(4'-methoxystyryl)pyridine was irradiated, an overall yield of 95% was obtained, with 64% being a single cyclobutane isomer, whereas irradiation of the analogous trifluoromethyl azastilbene 4-(4'-trifluoromethylstyryl)pyridine produced the major cyclobutane isomer in only 24% yield. On the basis of the effect of alkene polarization, it was argued that cation- π interactions are responsible for the increased yield and selectivity observed with solution-state irradiations of styrylpyridinium salts vs their uncharged counterparts.

Photolysis reactions in the solid state produce results markedly different from those in solution, with the styrylpyridine free bases forming only very low yields of cyclobutanes (<5%) and percent conversion to the dimer from the pyridinium salt varying greatly depending on the alkyl group and counterion used.^{27,28} While X-ray crystal structures were not obtained for the majority of these azastilbenes, the significant effect of counteranions on the dimerization yield suggests that changes in molecular packing might be at play and thus might be explained by the topochemical postulate. This presumption was reinforced by results with 1,2-bis(4-pyridyl)ethylenes and 1,2-bis(2-pyrazinyl)ethylenes, which demonstrated an inverse correlation between the distance separating the double bonds and the rate of dimerization,³⁰ and more recently by the solid-state photolysis of a wide array of 4-stilbazole HCl salts.³¹

While there are a few other examples of azastilbene solid-state photochemical reactions, a thorough literature search of the photodimerization of styrylpyrimidines revealed only three examples,^{32–35} one of which appears to be an accidental dimerization that occurred during a recrystallization.³⁴ The most pertinent of these reports compares the irradiation products from three different styrylpyrimidines, with the pyrimidine rings in various oxidation states, as well as those of various other heteroaromatic stilbenes.³³ Only in systems highly polarized by electron-withdrawing heteroaromatics were cyclobutanes produced in good yields and high selectivity, leading the authors to conclude that the polarity of the stilbene-type systems governs photoreactivity by directly influencing crystal packing.

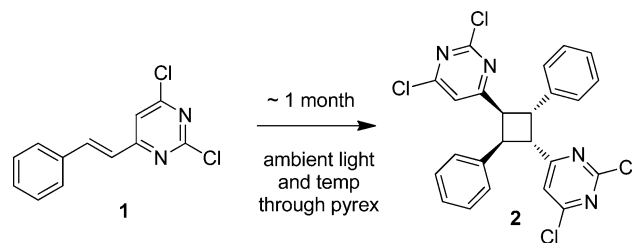
In this study, we determine the yield and regio- and stereoselectivity of the photodimerization of a variety of mono-, di-, and triazastilbenes in both the solid state and solution. Density functional theory and ab initio correlated calculations have been performed on each of the azastilbenes in order to determine dimer interaction energies, and these energies are correlated to the photochemical outcomes. While strong correlation exists between interaction energies and solution reaction rate and selectivity, photodimerization in the solid state is rationalized by consideration of the topochemical postulate and the concept of reaction cavity, as supported by X-ray crystal structure analysis of the photoreactive monomers.

RESULTS

Our interest in topochemically controlled reactions was triggered by the accidental discovery of the light-initiated dimerization of *trans*-2,4-dichloro-6-styrylpyrimidine (**1**) to form cyclobutane **2**, which occurred in the solid state over the course of approximately 1 month in a round-bottom flask

on the benchtop under ambient lighting and temperature (Scheme 1). Intrigued by the facile nature and complete

Scheme 1. Unanticipated Synthesis of Tetraaryl Cyclobutane 2



stereocontrol exhibited by this reaction, we attempted to replicate the photocycloaddition under more controlled conditions. Irradiation of 1 g of styrylpyrimidine **1** layered between two sheets of borosilicate glass with a water-cooled 450 W Hanovia medium-pressure mercury arc lamp gave complete conversion of the starting material in approximately 1.5 h, with similar retention of stereo- and regioselectivity. Milder light sources—a Rayonet reactor equipped with 8 W ultraviolet bulbs or a 250 W infrared sun lamp used in a light-reflective box—also efficiently converted **1** to **2**, with the sun lamp providing quantitative conversion of 50 mg of **1** to the cyclobutane in less than 40 min.

Solution-state photolysis was also performed on **1** with varying degrees of success. A 5 mg/mL solution of **1** in three different solvents, benzene, acetonitrile, and methanol, was irradiated in a photochemical reaction vessel with a water-cooled 450 W Hanovia medium-pressure mercury arc lamp for 4–5 h. The results of these trials, as measured by ¹H NMR of the crude reaction mixture, are shown in Table 1. This analysis is based on the integration and comparison of the vinyl and cyclobutyl protons of the various isomers formed during photolysis, each of which generally produces at least one unique signal that is adequately separated from those of the other isomers.

Figure 1 shows the five possible head-to-tail (htt) stereoisomers and eight possible head-to-head (hth) stereoisomers (including three pairs of enantiomers) that can be formed from the irradiation of **1**. Labeling of the isomers in both Table 1 and Figure 1 is according to IUPAC convention,³⁶ where *r* refers to the reference carbon (labeled with a small '1' in Figure 1) and *c* or *t* refers to the stereochemistry (cis or trans, respectively) of the group on subsequently numbered carbon atoms in relation to the substituent on the reference carbon. The analysis of the spectrum of each cyclobutane isomer, which is necessary for this type of examination, is described below and is given more extensively in the Supporting Information.

The results of the solution-state irradiations differ markedly from those obtained from the solid-state examples above. Despite prolonged irradiation times, photolysis in benzene or acetonitrile gives mostly *trans*/*cis* isomerization, with *cis*-2,4-dichloro-6-styrylpyrimidine (*cis*-**1**) as the major product (52% and 45%, respectively). In both solvents, cyclobutane dimers are minor products (12% in benzene and 17% in acetonitrile), and while there is some selectivity for the htt *r*-*ctt* isomer **2** relative to the other cyclobutanes formed (65% and 45% for benzene and acetonitrile, respectively), this fails to approach the essentially exclusive formation of **2** obtained from the lower-power solid-state irradiations. Irradiation in methanol

Table 1. Solid- and Solution-State Irradiation Products (%) of 2,4-Dichloro-6-styrylpyrimidine (**1**) Presented in Mass Percent of the Crude Product Mixture As Determined by Analysis of the Alkene/Cyclobutane Proton Peaks in ^1H NMR

solvent	diazastilbene		head-to-tail cyclobutane isomers					head-to-head cyclobutane isomers					red/add
	<i>trans</i>	<i>cis</i>	<i>r-ctt</i>	<i>r-ctc</i>	<i>r-ctc</i>	<i>r-tct</i>	<i>r-ccc</i>	<i>r-ctt</i>	<i>r-tcc</i>	<i>r-ctc</i>	<i>r-tct</i>	<i>r-ccc</i>	
solid state	0	0	100	0	0	0	0	0	0	0	0	0	0
Ph-H	36	52	7	1	0	1	0	1	0	0	1	0	0
ACN	38	45	8	3	0	3	0	2	0	0	2	0	0
MeOH	24	48	3	2	0	2	0	2	0	0	2	0	23

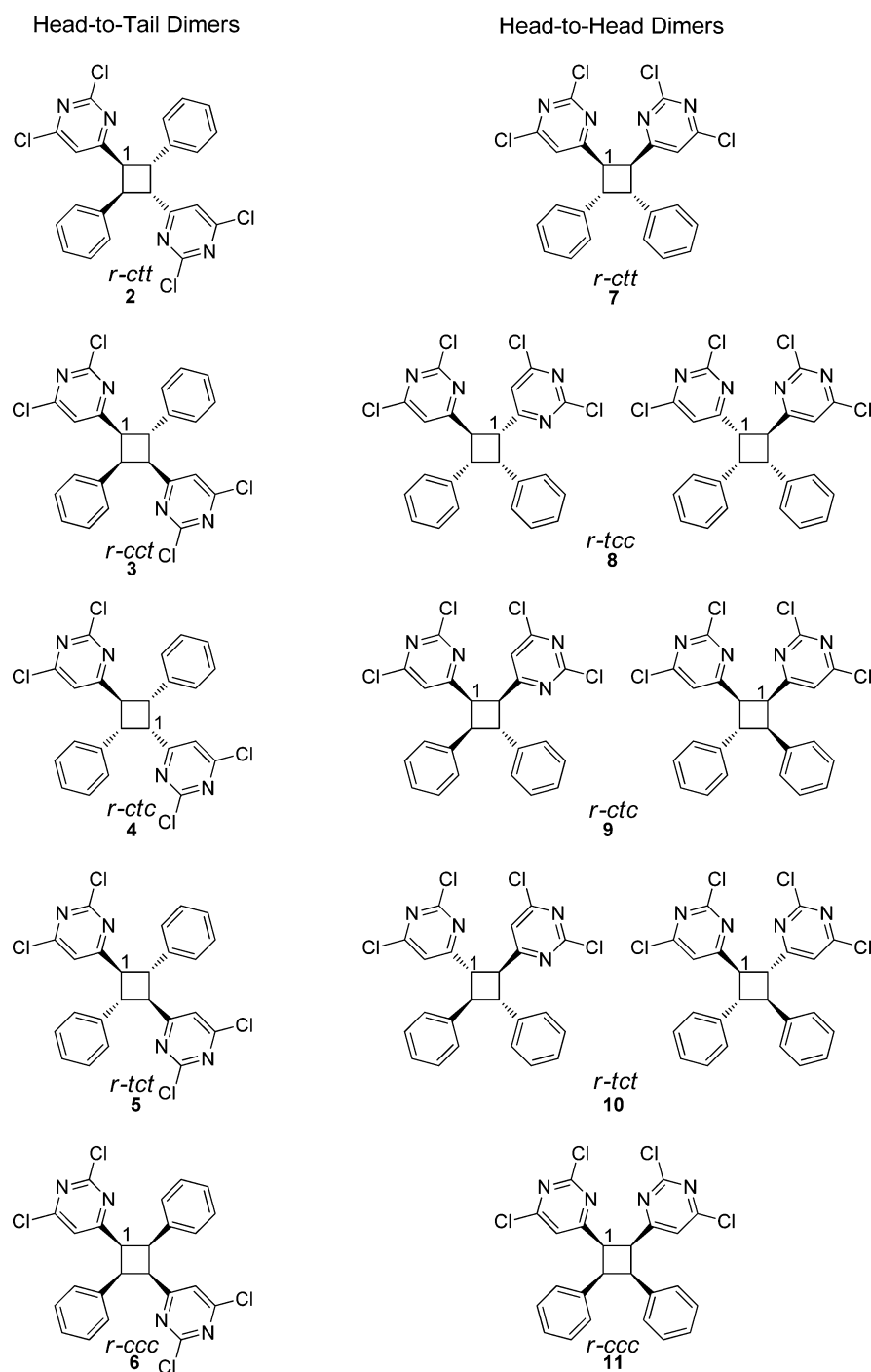


Figure 1. Thirteen regio- and stereoisomers that can hypothetically arise from the irradiation of **1**. The reference (*r*) carbon is denoted by the small “1”.

provides similar results, with the additional appearance of large amounts of alkene reduction and solvent addition products, a

conversion known from irradiation of other azastilbenes in protic solvents.³⁷ Nevertheless, dimer formation remains

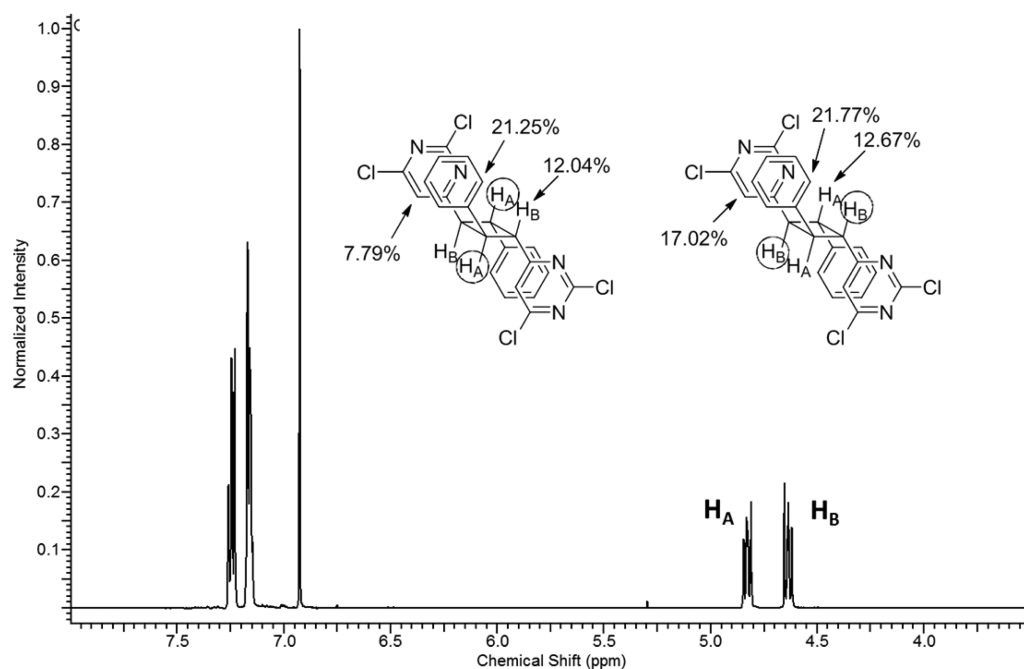


Figure 2. ^1H NMR (500 MHz, CDCl_3) spectra and percent NOEs for the htt *r-ctt* dimer **2**. The irradiated protons for each structure are circled and the percent NOEs based on this proton are indicated.

comparable at 15%, and while the htt *r-ctt* isomer **2** is still the dominant cyclobutane, it represents only 28% of the total cyclobutanes.

Isolation and Elucidation of the Photoproducts of *trans*-2,4-Dichloro-6-styrylpyrimidine. To isolate adequate quantities of the minor cyclobutane isomers for full characterization, we combined chromatographic fractions from the above solution-state irradiations. Solid-state irradiation (4 h, medium-pressure mercury lamp) of the *cis*-2,4-dichloro-6-styrylpyrimidine isolated from the solution-state irradiations also helped provide additional cyclobutane products containing appreciable quantities of the minor cyclobutane dimers. Extensive chromatographic separations of these products eventually produced pure or nearly pure samples of 8 of the 10 theoretical diastereomers and enantiomeric pairs (compounds **2–5** and **7–10**).

To confirm its regio and stereochemistry, a crystal structure of the initial htt *r-ctt* cyclobutane **2** was obtained (see Figure S1 in the Supporting Information). Nuclear Overhauser effect (NOE) spectra of **2** allowed us to make ^1H NMR assignments of the cyclobutyl protons. The percent NOEs for each cyclobutyl proton of **2** along with the corresponding parent ^1H NMR spectrum are shown in Figure 2. With the regio- and stereochemistry of dimer **2** firmly established, NOE analysis became the basis for structural determination and ^1H NMR peak assignment of the other cyclobutanes. This approach permitted confident identification of five of the seven remaining isolated isomers, with some ambiguity associated with differentiation between the two remaining cyclobutanes (compounds **8** and **9**). The rationale behind the assignment of each ^1H NMR spectral/compound pair is described in detail in the Supporting Information. These assignments are used throughout the remainder of the paper.

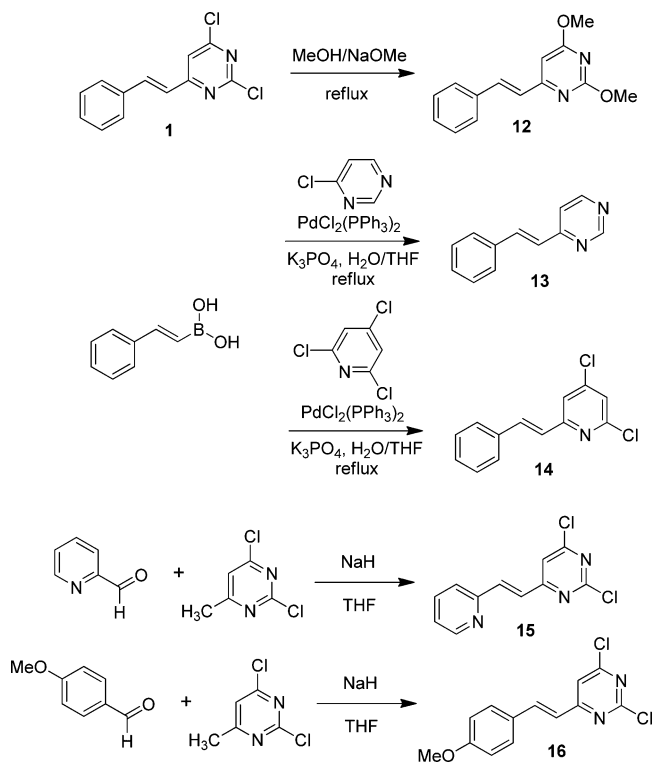
Synthesis and Solid-State Irradiation of Azastilbene Derivatives of Styrylpyrimidine **1.** We next explored how varying the electron-withdrawing and -donating nature of the two aromatic rings affected the rate of solid-state photo-

cycloaddition of these compounds. On the basis of earlier precedent for styrylpyridines and styrylpyrimidines,^{29,33} we hypothesized that more polarized compounds would interact with increasing strength through head-to-tail π stacking, producing tightly packed crystals that are readily photoreactive. Conversely, we expected that less polarized compounds would either fail to undergo photocycloaddition or react only slowly, with an accompanying loss of stereo- and regioselectivity. To test this hypothesis, we prepared a set of five additional azastilbenes bearing electron-withdrawing (chlorine), electron-donating (methoxy), or electron-neutral (hydrogen) substituents on the pyrimidine or pyridine rings. The phenyl substituent was also replaced in two of the derivatives by a methoxyphenyl or pyridine moiety.

The synthesis of the azastilbenes was straightforward and in each case proceeded in only a single step from readily available starting materials (Scheme 2). *trans*-2,4-dimethoxy-6-styrylpyrimidine (**12**) is formed by the $\text{S}_{\text{N}}\text{Ar}$ reaction of **1** in a 25% solution of NaOMe in methanol, heated to reflux overnight. *trans*-6-Styrylpyrimidine (**13**) and *trans*-2,4-dichloro-6-styrylpyridine (**14**) are synthesized by simple Suzuki–Miyaura cross-couplings from *trans*-styrylboronic acid and the corresponding heteroaryl chlorides. Finally, the triazastilbene **15** and 4-methoxystyrylpyrimidine **16** are produced from the base-catalyzed condensation of 2,4-dichloro-6-methylpyrimidine with the appropriate aryl aldehydes.

To adequately probe the relationship between π system polarization and topochemically controlled reactivity, we prepared an irradiation facility that provided uniform light intensity and temperature. Due to the relatively low melting point of some of the diazastilbenes, it was especially important to ensure even cooling of the reaction sample. Thus, a water-cooled borosilicate glass plate was created, upon which the ground, recrystallized sample was spread and then covered with a second borosilicate glass plate. To aid in cooling the reaction mixture, we selected a “cool” light source of intensity comparable to that of the 250 W sun lamp commonly used

Scheme 2. Synthesis of Azastilbene Derivatives



in irradiations: a 68 W compact fluorescent light (300 W incandescent equivalent, 2700 K color temperature). This source converted 50 mg of **1** into **2** in less than 30 min.^{38,39} When the reaction is performed in an aluminum foil-encased enclosure, this simple setup allows for an approximately room temperature irradiation in which the air temperature does not exceed 30 °C and the surface of the water-cooled plate has a constant temperature of 23–25 °C.

Using this setup, we performed irradiations on 45–50 mg of recrystallized material for each of the six *trans*-azastilbenes (**1**, **12**–**16**), as well as on *cis*-2,4-dichloro-6-styrylpyrimidine (**1**), with time points taken at 10 min intervals for the first 2 h and at 0.5–1 h intervals thereafter. Each sample was analyzed by ¹H NMR, and in most cases, the eight expected cyclobutane isomers could be differentiated, on the basis of the ¹H NMR assignments made previously for the various isomers of compound **2**. An example of peak assignments for the crude irradiation spectrum of compound **13**, showcasing the ability to distinguish between photoproducts using ¹H NMR, is shown in Figure 3 (spectra for other irradiations are available in the Supporting Information). For each photolysis, the percent composition of every component in the reaction mixture was determined from the peaks arising from the vinylic protons of the starting material (*cis*- and *trans*-vinylic as well as cyclobutyl peaks). These values were then plotted vs time, and an exponential least-squares curve was fitted to each data set (see Figure 4 for photolysis curves of **1** and **15** and the Supporting Information for the irradiation plots of the remaining compounds).

The half-lives ($t_{1/2}$) for the formation of each component in the final photolysis mixture, along with the associated values for all combined cyclobutane isomers, are shown in Table 2. Table 3 gives the percent composition of each component of the reaction mixtures at the final time point for each photolysis. A study of these tables reveals somewhat contradictory trends. On the basis of our initial hypothesis, we expected those systems that are adequately polarized (i.e., having one electron-withdrawing and one electron-donating ring) would provide the *htt r-ctt* isomer preferentially. Additionally, we expected that the more polarized the azastilbene, the more rapid the reaction (smaller $t_{1/2}$). While the dichlorostyrylpyridine **14** reacted exclusively to form the *htt r-ctt* isomer with a satisfactory rate ($t_{1/2}$ ca. 4 times that for the similar reaction of **1**), it was unique among the set of derivatives. Even the highly polarized 4'-methoxystyrylpyrimidine **16** failed to selectively produce the *htt*

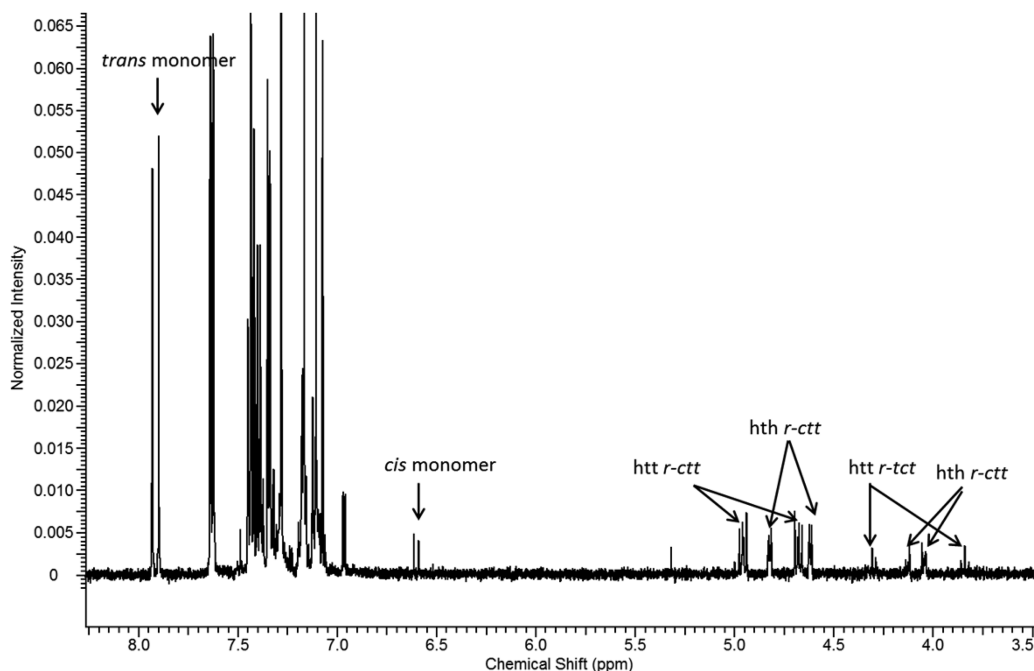


Figure 3. ¹H NMR (500 MHz, CDCl₃) of the crude reaction mixture for the solid-state irradiation of **13** at 24 h.

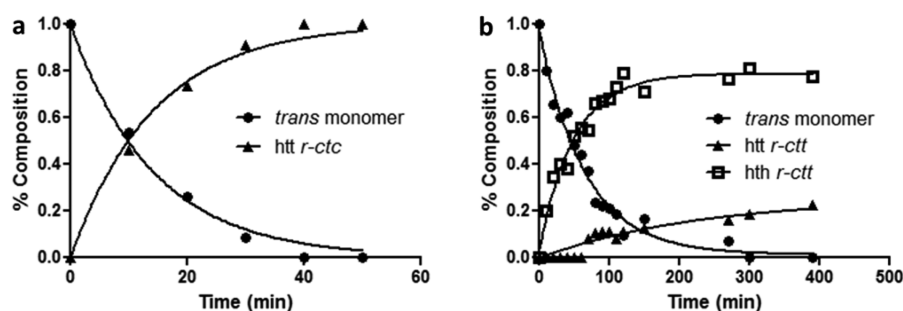


Figure 4. Photolysis time courses with fitted exponential curves for (a) *trans*-2,4-dichloro-6-styrylpyrimidine (**1**) and (b) *trans*-2,4-dichloro-6-(2-pyridin-2-yl)vinylpyrimidine (**15**).

Table 2. $t_{1/2}$ Values for the Photoproducts of the Solid-State Irradiation of Azastilbenes **1** and **12**–**16**

azastilbene	<i>cis</i> ^b	$t_{1/2}$ of formation (min) ^a				
		comb CBS ^c	htt		hth	
			<i>r-ctt</i>	<i>r-tct</i>	<i>r-ctt</i>	<i>r-tct</i>
1		9.8	9.8			
12		14 200	28800		28400	
13	498	1994	6730	>10 ⁵	3850	19700
14		39.1	39.1			
15		45.4	160		34.2	
16		201	331		243	
<i>cis</i> - 1 ^d	N/A	213	213			

^aIsomers not reported in the table were not observed upon photolysis.

^bRespective *cis*-azastilbene. ^c $t_{1/2}$ calculated from curve formed by total percent composition of all cyclobutanes in the reaction mixture. ^d*cis*-2,4-Dichloro-6-styrylpyrimidine.

r-ctt isomer (ca. 39% conversion, $t_{1/2}$ ca. 33 times that of **1**) and instead formed the hth *r-ctt* compound as the major product. Surprisingly, the photolysis of the significantly less polarized triazastilbene **15** proceeded 4 times as quickly as that of **16**, although it did favor formation of the hth dimer more strongly (81.3 vs 18.7% for the hth and htt *r-ctt* dimers, respectively).

In contrast to the solid-state irradiations with the highly polarized stilbene systems, the azastilbenes designed to have reduced polarity across the conjugated π system (**12** and **13**) reacted as expected, with very little conversion to the htt *r-ctt* dimer, even with extended irradiation times. The dimethoxy-substituted compound **12** was especially inert to photolysis, forming the htt *r-ctt* dimer in only 4.7% yield after 24 h. As with the initial irradiation of **1**, essentially no *cis*/*trans* isomerization

took place in the crystalline material. Only photolysis of **13** produced a small amount of the *cis*-styrylpyrimidine (6.5%) after 24 h.

Molecular Modeling of Azastilbene Interactions.

While chemical intuition allows for ordering of the azastilbenes on the basis of polarity across the π system (**16** > **1** > **14** > **15** > **13** > **12**), π stacking is an effect mediated by electronic effects more subtle than simply oppositely paired electrostatic charge.^{40,41} Consequently, it is more difficult to predict how increasing the electron-withdrawing and/or -donating nature of the aryl rings would affect the π stacking of the azastilbenes. To provide a more quantitative understanding of this stabilization of the azastilbenes, M06-2X density functional and correlated ab initio MP2 calculations were performed. All geometries were optimized with the M06-2X functional and 6-31G(d,p) basis set in Gaussian 09⁴² using an ultrafine integration grid⁴³ in the gas phase. Monomers and π -stacking “dimers” were oriented in either a head-to-tail or head-to-head manner, with the crystal structures described below acting as the starting point for the dimer geometry optimizations. All stationary points were verified as minima by vibrational normal mode inspection. Energies reported are M06-2X/6-311+G(2d,p)//M06-2X/6-31G(d,p). Interaction energies reported are relative to separated monomers and are corrected for basis-set superposition error. Spin component scaled MP2 (SCS-MP2) energies were computed by scaling the $\alpha\beta$ and $\alpha\alpha/\beta\beta$ MP2 correlation energies by $1/3$ and $6/5$, respectively.⁴⁴

The M06-2X and SCS-MP2 interaction energies for the azastilbene dimers are given in Table 4 and differ by an average of only 0.8 kcal/mol. The trends and relative changes in binding energy across the two methods are nearly identical.

Figure 5 shows a plot of the $t_{1/2}$ values of htt *r-ctt* dimer formation versus the SCS-MP2 interaction energies of the six

Table 3. Percent Composition of the Photoproducts of the Solid-State Irradiation of Azastilbenes **1** and **12**–**16**

azastilbene	time (min)	composition at end of irradiation (%) ^a						
		trans	<i>cis</i> ^b	comb CBS ^c	htt		hth	
					<i>r-ctt</i>	<i>r-tct</i>	<i>r-ctt</i>	<i>r-tct</i>
1	40	0	0	100	100	0	0	0
12	1440	90.5	0	9.5	4.7	0	4.8	0
13	1440	55.9	6.5	37.5	15.4	5.8	10.4	6.0
14	180	0	0	100	100	0	0	0
15	300	0	0	100	18.7	0	81.3	0
16	540	4.0	0	96.0	38.7	0	57.3	0
<i>cis</i> - 1 ^d	420	0	0	100	100	0	0	0

^aIsomers not reported in the table were not observed upon photolysis. ^bRespective *cis*-azastilbene. ^cPercent composition of all cyclobutanes in the reaction mixture. ^d*cis*-2,4-Dichloro-6-styrylpyrimidine.

Table 4. Azastilbene Interaction Energies

azastilbene	interaction energy (kcal/mol)	
	M062X	SCS-MP2
1	-15.8	-17.0
12	-6.4	-6.3
13	-11.8	-12.4
14	-14.8	-15.9
15	-14.2	-15.2
16	-17.8	-18.9

azastilbenes. On the basis of the presumption that compounds which exhibit a larger binding energy should pack more tightly in the head-to-tail configuration, one would expect that azastilbenes that release more energy upon interaction would produce the htt *r-ctt* cyclobutane more rapidly in greater yield. While this holds true for compounds 1 and 12–14, monomers 15 and 16 do not react as expected in the solid state (Figure 5b,c). Due to the large interaction energy of azastilbene 16 (–18.8 kcal/mol), we anticipated that the reaction rate and yield for the htt dimer would be comparable to or higher than that of compound 1 (interaction energy –17.0 kcal/mol). Nonetheless, the opposite is true: the solid-state photolysis of 16 forms the htt *r-ctt* dimer at a rate 300 times slower than that of 1 and provides the htt *r-ctt* dimer in only 39% yield, whereas 1 undergoes quantitative conversion to 2. Furthermore, on the basis of the close binding energies exhibited by 14 and 15, one would expect these two to have similar $t_{1/2}$ values for the formation of the htt *r-ctt* dimers. As with 16, compound 15 fails to perform as anticipated and reacts to form the htt dimer at a rate 6 times slower than does 14. More striking is the lack of regioselectivity observed in the irradiation of 15, which produces the htt dimer in only 19% yield, while 14 is quantitatively converted to the htt *r-ctt* cyclobutane.

In addition to binding energies, electrostatic potentials were calculated for each monomer and head-to-tail π -stacking pair, and these are projected on an isodensity surface in Figure 6 (blue, +0.02 hartree; red, –0.02 hartree). Unfortunately, visual inspection of these surfaces fails to provide significant insight into which systems are more polarized; while a difference in electrostatic potential obviously exists across the aromatic rings of each compound, from the ESPs it is impossible to grade this level of polarity. More visually satisfying is the increase of polarity observed across monomers as they interact in the htt dimer formation (bottom row of Figure 6). This change in electrostatic potential is anticipated as the π systems begin to feed into one another, accentuating the charge differential across the azastilbene.

Crystal Analysis and Photoreactivity of *trans*-Azastilbenes. To understand the disconnect between the binding energies and reactivity of compounds 15 and 16, single-crystal X-ray structures of the azastilbene monomers 1 and 16 were obtained and compared. As anticipated from both the experimental results and computation work, 2,4-dichloro-6-styrylpyrimidine (1) packs in an array of infinite columns in a head-to-tail manner (Figure 7). There are two unique columns contained in each unit cell; these alternate with distances between the monomers being either 3.543 or 3.775 Å. The short distance and planarity between the alkene double bonds suggest that the [2 + 2] photocycloaddition between monomers of 1 should proceed under topochemical control, and this is indeed the case (as described above).

The X-ray crystal structure of azastilbene 16 is more intriguing. On the basis of the push–pull nature of the aromatic rings and the large interaction energy exhibited by the head-to-tail dimer of 16, we expected crystal packing to mimic that of 1. Nevertheless, the 4'-methoxyazastilbene packs in a head-to-head array with multiple infinite columns contributing to the unit cell (Figure 8). The crystal analysis of 16 displays

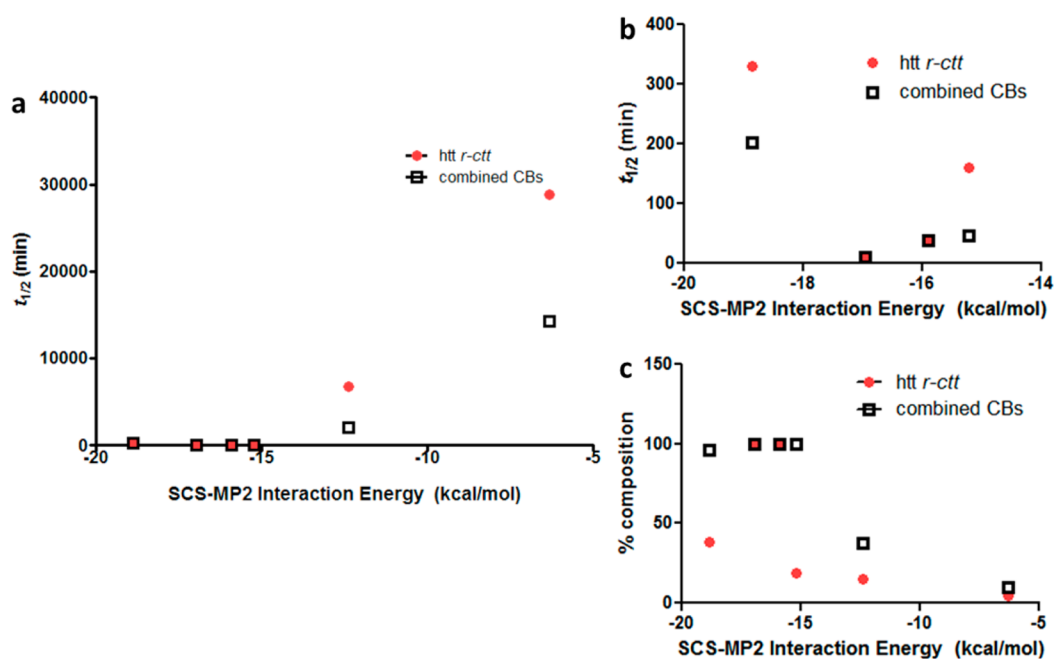


Figure 5. Correlation between SCS-MP2 interaction energies and the formation of cyclobutanes under solid-state irradiation conditions: (a) $t_{1/2}$ vs interaction energy; (b) enlargement of the plot showing $t_{1/2}$ vs interaction energy with only the first four points shown; (c) percent composition of cyclobutanes at final irradiation time vs interaction energy.

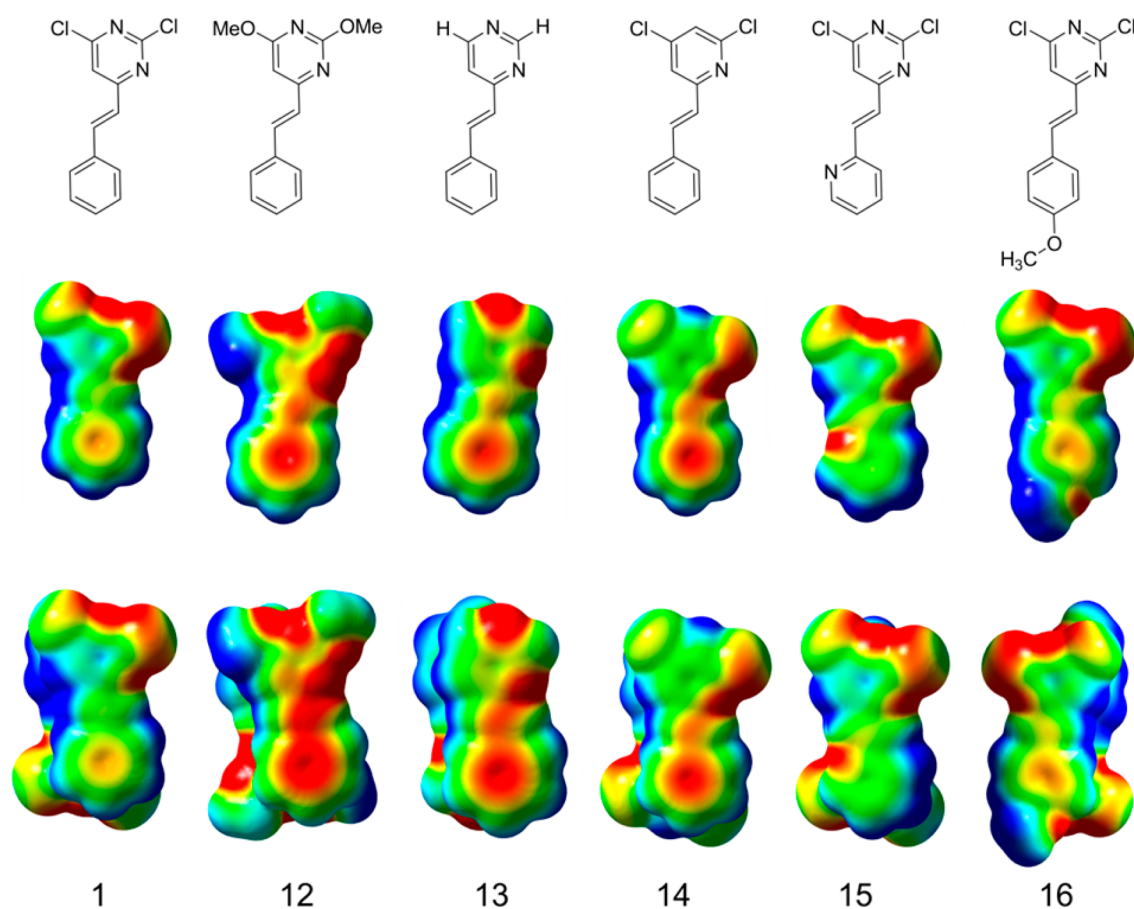


Figure 6. Electrostatic potential surfaces of azastilbenes (middle row) and their head-to-tail interacting dimers (bottom row).

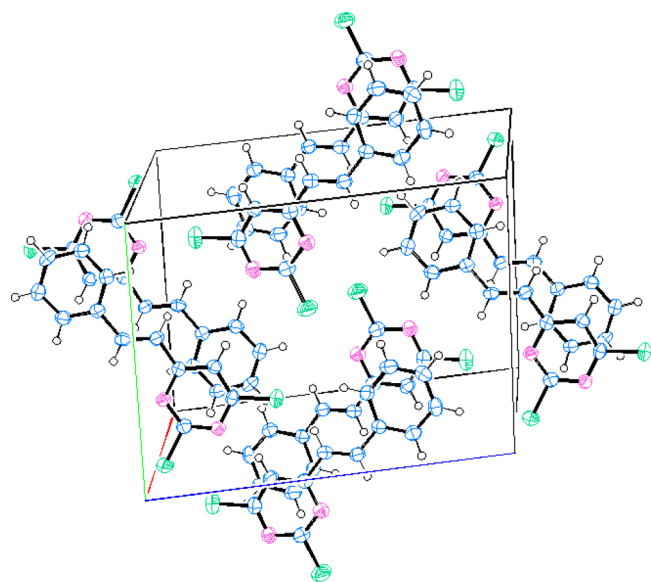


Figure 7. X-ray crystal structure of *trans*-2,4-dichloro-6-styrylpyrimidine (**1**).

only a single interalkene distance of 4.164 Å. This places the reacting double bonds at the limits of the distance in which the topochemical principles are considered to operate (4.2 Å). Nonetheless, with the crystal structure of **16** in hand, the regio- and stereochemistry observed upon its solid-state irradiation can readily be explained. Indeed, it appears that photolysis of

16 also proceeds under quasi-topochemical control, producing the *hth r-ctt* dimer preferentially (57.3% conversion).

Crystal Structure of *cis*-2,4-Dichloro-6-styrylpyrimidine. As shown in Tables 2 and 3, the solid-state irradiation of *cis*-2,4-dichloro-6-styrylpyrimidine (**cis-1**) produces **2** in yields equivalent to that from the irradiation of *trans*-2,4-dichloro-6-styrylpyrimidine (**1**), albeit at a significantly decreased rate ($t_{1/2}$ of 213 min vs 9.8 min for the *trans* isomer). There are two possible routes for formation of the *hth r-ctt* dimer from the crystalline *cis*-azastilbene. **cis-1** might crystallize in such a manner that the reacting double bonds are parallel to each other, with the aryl rings of each alternating monomer oriented away from one another; if the [2 + 2] photocycloaddition then proceeded under topochemical control, cyclobutane **2** would be formed selectively (top pathway of Scheme 3). Alternatively, crystalline **cis-1** might first undergo light-initiated *cis/trans* isomerization to **1**, which then reorients to form microcrystals that give rise to **2** (bottom pathway of Scheme 3).

To differentiate between these two pathways, we obtained an X-ray crystal structure of the **cis-1** starting material. As shown in Figure 9, the unit cell of **cis-1** also contains multiple infinite columns which are packed in such a manner that the alkenyl double bonds are parallel to one another. Nonetheless, if the stereochemistry of the photoproducts was determined by the solid-state molecular packing, one would expect the *hth r-ccc* isomer to be produced, not the *hth r-ctt* cyclobutane. Additionally, measurement of the space between the reacting double bonds in the **cis-1** crystal shows that they are separated by 5.131 Å, too large for cycloaddition without significant perturbation of the crystal lattice. Thus, formation of **2** from

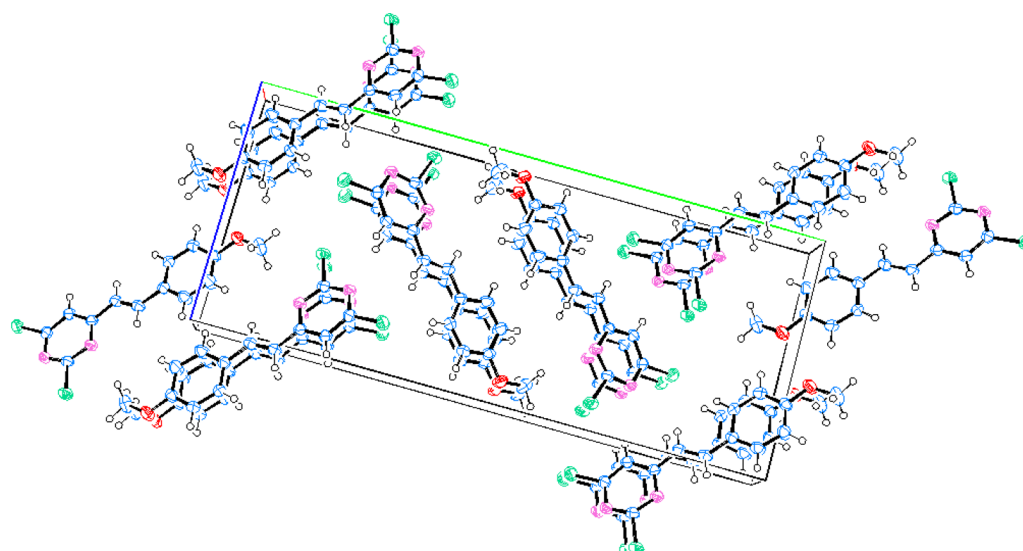
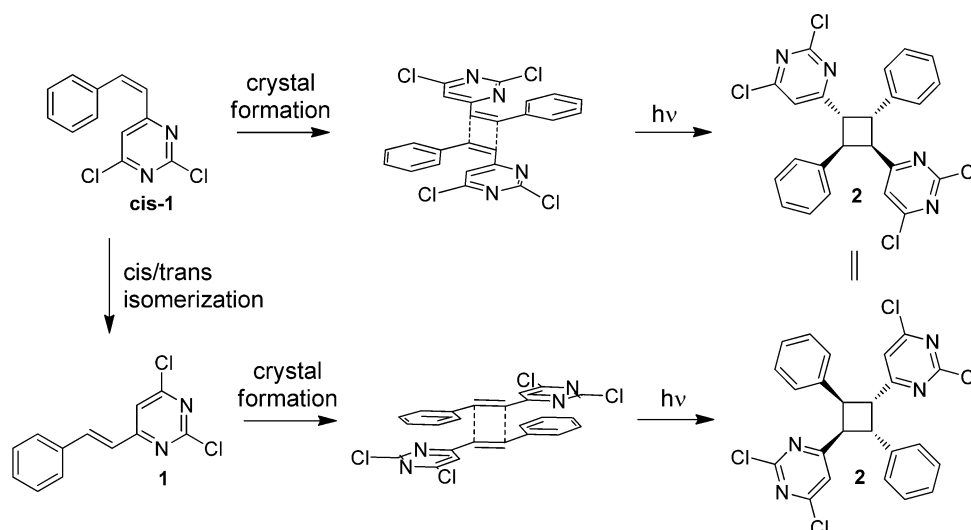


Figure 8. X-ray crystal structure of *trans*-2,4-dichloro-6-(4-methoxystyryl)pyrimidine (**16**).

Scheme 3. Formation of Cyclobutane **2** from *cis*-2,4-Dichloro-6-styrylpyrimidine



cis-**1** cannot be proceeding under topochemical control; therefore, the alternate pathway must be considered.

Additional evidence for *cis*/*trans* isomerization in the solid-state photolysis of *cis*-**1** is apparent in the presence of *trans* isomer **1** in the reaction mixture after as little as 20 min of irradiation (see Figure S18e, Supporting Information). The amount of **1** remains at a fairly constant level (3–10%) throughout the irradiation but disappears near the completion of the reaction. The absence of crystal packing suitable for formation of the *hct* *r-ctt* cyclobutane, and the confirmed presence of **1** in the reaction mixture, strongly suggest that the conversion of *cis*-**1** to **2** proceeds through the *trans*-azastilbene intermediate. While visual inspection throughout the water-cooled irradiation of *cis*-**1** shows no observable solid-to-liquid transformation, it is possible that the initial *cis*/*trans* isomerization is expedited by microscopic melting, facilitated by the relatively low melting point of *cis*-**1** (47–48 °C).

Solution-State Irradiation of Azastilbene Derivatives.

From the X-ray crystal structure of **16**, it became clear that the stereo- and regiochemistry observed upon irradiation of this compound were due to its molecular packing in the solid state.

This packing overcame the inherent polarity and associated energetic preference for head-to-tail interaction demonstrated in the gas-phase calculations of the 4'-methoxyazastilbene (similar considerations likely apply to the triazastilbene **15**). We wanted to investigate whether this bias toward head-to-head photoproducts for **15** and **16** could be reversed by irradiation in solution, which would eliminate the constraints enforced by the structured crystal lattice. To this end, 40 mM solutions of each azastilbene in CDCl₃ were prepared and subsequently irradiated in sealed borosilicate NMR tubes. Photolysis was accomplished using the same arrangement as described for the solid-state irradiations, and all of the azastilbene samples were irradiated simultaneously so as to minimize variability. The percent composition of each sample after 24 h of photolysis is shown in Table 5 (see the Supporting Information for spectra of the solution-state irradiation product mixtures).

As expected, the solution-state irradiations resulted predominantly in *trans*/*cis* isomerization of the azastilbene rather than cycloaddition. For all compounds except **15** and **16**, the *cis* monomer was the predominant component of the reaction mixture at 24 h. Additionally, there was a loss of regio- and

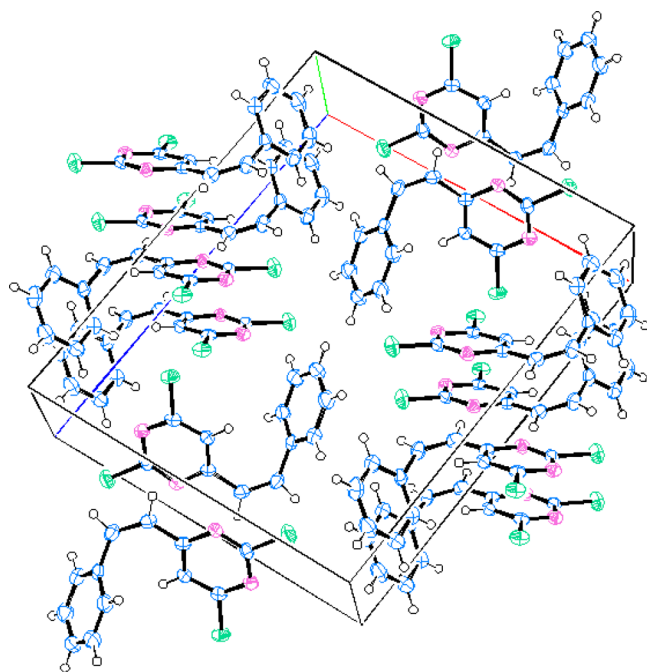


Figure 9. X-ray crystal structure of *cis*-2,4-dichloro-6-styrylpyrimidine.

stereoselectivity for most of the azastilbene samples. This was especially striking for **1** and **14**, which, in the solid state, were quantitatively converted to the *htt r-ctt* isomer. While the *htt r-ctt* isomer continues to be the major cyclobutane product, the formation of multiple other isomers attests to the role that topochemical control plays for these compounds in the solid state. In addition to the *htt r-tct* and *hth r-ctt* and *r-tct* dimers observed as products of the solid-state irradiations, the solution-state irradiations also produced varying amounts of the previously identified *htt r-ctt* and *r-ctc* and *hth r-tcc* and *r-ctc* isomers. Because the ^1H NMR peaks of the *hth r-ctt* and *r-ctc* isomers as well as the *htt r-ctt* and *r-ctc* isomers overlap, the percent compositions of these compounds in Table 5 are combined. Intriguingly, in four of the six samples a ninth cyclobutane dimer, the *htt r-ccc* isomer, was found. This assignment is based on the presence of two distinct doublets located between δ 3.9 and 4.3 in the ^1H NMR of the product mixture of four of the six azastilbenes (in the photolysis of **13** these peaks presumably overlap to form an apparent quartet at δ 4.04). The assignment of the *htt r-ccc* isomer to these peaks is negated by the splitting pattern (doublet vs triplet). The presence of multiple methoxy peaks in the spectra of the

product mixture from irradiation of **12** and **16** makes it impossible to confirm or deny the presence of the *hth r-ccc* dimer. It should be noted that irradiation of triazastilbene **15** leads to formation of insoluble photoproducts which preclude the accurate measurement of the reaction components by NMR. Two additional products of note include the possible formation of the *htt r-ccc* dimer from **14** (on the basis of an otherwise unexplained singlet at δ 4.01) and a benzo[*f*]-quinazoline, formed upon the irradiation of **12**. Benzo[*f*]-quinazoline is a well-known irradiation product of diazastilbenes.^{45–48}

Regardless of the presence of multiple cyclobutane isomers in the solution-state irradiation mixtures, in every instance except for compound **15**, the predominant product was the *htt r-ctt* isomer. The percent composition of the *htt r-ctt* adducts as well as of the total combined cyclobutane products from the azastilbene solution irradiations are displayed, plotted against the SCS-MP2 binding energy calculated for each compound in Figure 10 (compound **15** has been excluded from this analysis

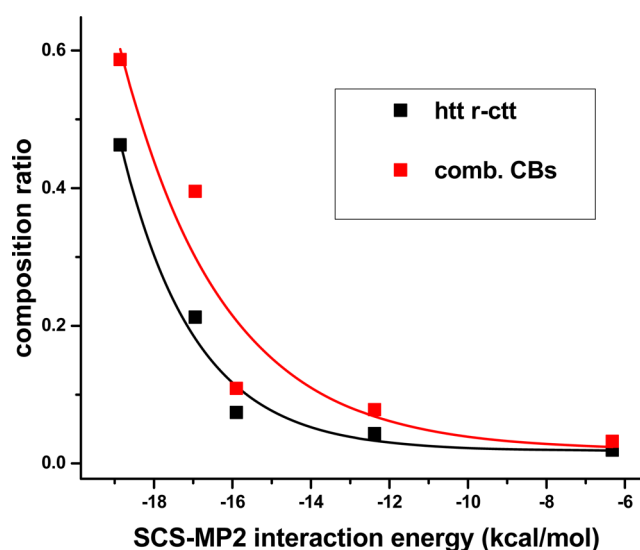


Figure 10. Correlation between SCS-MP2 interaction energies and the formation of cyclobutanes under solution-state irradiation at 24 h.

based on the insolubility of its photoproducts). In contrast to the solid-state photolysis, the solution irradiations display a consistent relationship between the binding energy of the azastilbenes and the yield of the *htt r-ctt* dimer, and an exponential least-squares curve fitting provides a coefficient of determination (R^2 value) of 0.96. A similar analysis of the

Table 5. Percent Composition of Solution-State Irradiation Mixture of Azastilbenes at 24 h

azastilbene	composition (%)											peri-cyclic pdt ^c	comb CBs ^d
	<i>trans</i> ^a	<i>cis</i> ^b	htt				hth						
			<i>r-ctt</i>	<i>r-ctt</i> + <i>r-ctc</i>	<i>r-tct</i>	<i>r-ccc</i>	<i>r-ctt</i>	<i>r-tcc</i> + <i>r-ctc</i>	<i>r-tct</i>	<i>r-ccc</i>			
1	29.9	30.6	21.3	1.9	5.2	0.0	4.9	0.0	4.0	2.3	0.0	39.5	
12	32.5	61.2	1.9	0.1	0.0	0.0	0.5	0.6	0.0	0.0	3.1	3.2	
13	35.0	57.2	4.3	0.5	0.3	0.0	1.1	0.0	0.1	1.6	0.0	8.0	
14	39.9	49.2	7.4	0.0	0.6	0.6	1.3	0.0	0.0	1.0	0.0	10.9	
15^e	65.5	22.9	0.0	0.0	3.5	0.0	2.3	0.0	4.3	1.5	0.0	11.6	
16	27.3	14.0	46.3	1.7	5.0	0.0	4.6	0.0	1.1	0.0	0.0	58.7	

^aRespective *trans*-azastilbene. ^bRespective *cis*-azastilbene. ^cRespective benzo[*f*]quinolone or benzo[*f*]quinazoline. ^dPercent composition of all cyclobutanes in the reaction mixture. ^eDecomposition/precipitation of SM/pdt upon irradiation.

percent composition of all the combined cyclobutanes in each reaction mixture produces a somewhat worse fit, with an R^2 value of 0.83, reflecting the expectation that the head-to-tail binding energy provides a better predictive measure of htt *r-ctt* dimer formation than that of cyclobutane formation as a whole.

DISCUSSION

The range of solid-state photochemical results we have presented here is generally consistent with the conclusions made by Schmidt and co-workers when they first presented their topochemical postulates.^{8–11,49} Namely, the crystal structure of *trans*-2,4-dichloro-6-styrylpyrimidine (**1**) displays a molecular packing in which the double bonds undergoing [2 + 2] photocycloaddition are parallel to one another and are separated by less than 4.0 Å. As would be expected from this orientation, the htt *r-ctt* dimer **2** is formed in quantitative yield in a short amount of time with even moderate-intensity light sources ($t_{1/2}$ of less than 10 min). When azastilbenes of similar or increased polarity across the π system were irradiated in the solid state, the results initially proved contradictory. While the less polarized *trans*-2,4-dichloro-6-styrylpyridine (**14**) also quantitatively produced the htt *r-ctt* cyclobutane, albeit with a longer half-life than for the reaction of **1**, the similarly polar triazastilbene **15** and significantly more polarized 4'-methoxy-styrylpyrimidine **16** preferentially produced the hth *r-ctt* dimer.

X-ray structural analysis of **16** sheds light on these results, as it shows a consistent head-to-head arrangement of infinite columns of azastilbene monomers with an interalkene distance just under 4.2 Å. Further inspection of the crystal structure reveals multiple weak hydrogen bonds stabilizing this arrangement. Most notable of these are the intracolumnar methoxy C–H to O (2.613 Å) and methoxy C–H to π (2.860 Å) interactions. There are two additional intercolumnar weak hydrogen bonds: pyrimidinyl C–H to N (2.719 Å) and phenyl C–H to O (2.67 Å). Weak hydrogen bonding has been studied extensively through crystal structure analysis as well as by computations (see the reviews by Steiner and Desiraju).^{50–52} The distances measured for the weak interactions in the crystal structure of **16** (all <3 Å) suggest structurally significant bonding, and while it is difficult to assign energy values to any single interaction, other examples of C–H to O, C–H to π , and C–H to N bonds have been calculated to range from ≤ 1 to >2 kcal/mol. Consequently, it is not surprising that these weak hydrogen bonds in aggregate are able to overcome the energetically less favorable head-to-head π -stacking conformation (15.1 vs 18.9 kcal/mol binding energy for the hth vs htt dimers).

Although the topochemical postulate can be used to explain the hth *r-ctt* isomer as the major photoproduct of solid-state **16** (57.3% conversion), it is more difficult to justify the large amount of the htt *r-ctt* isomer formed from this reaction (38.7%). Two main explanations for the loss of topochemical control have been presented in the literature.^{8,30} Both argue that nontopochemical isomers are produced at defects in the crystal. In one view these defects are present in the crystal at the beginning of irradiation and are continually propagated as the nontopochemical isomer forms. The other argument concludes that formation of topochemical dimers causes local disruption in the crystal lattice. This eventually produces defects in which a new crystal phase is formed during the photolysis, from which the nontopochemical isomer arises. The

presence of the htt isomer upon irradiation of **16** could be justified according to either of these posits.

Extension of this reasoning to compounds **14** and **15** suggests that photoproduct formation proceeds from the head-to-tail and head-to-head crystal forms, respectively. Although the absence of a methoxy group on **14** and **15** negate the possibility of the intracolumnar C–H to O and methoxy C–H to π bonds pertinent to **16**, the unique presence of a pyridine in these compounds may predispose to stronger C–H to N hydrogen bonds, leading to unanticipated packing orientations and the observed irradiation results.

As described here, we have attempted to correlate the polarity of interacting π systems with their photoreactivity in the solid state. To better gauge the effect of different aryl substituents on polarization of the azastilbenes, DFT and MP2 calculations were performed in both the monomer and “dimer” states. These calculations provided interaction or binding energies which could then be correlated to the azastilbene photoreactivity. Gratifyingly, the trends in binding energy mimicked those that would have been predicted from an intuitive analysis of the stilbenes, on the basis of generally accepted electron-withdrawing and electron-donating properties of the aryl rings. More importantly, these calculations provide quantitative values that can be compared to the rates and percent compositions obtained from the various photolysis reactions.

We hypothesized that compounds exhibiting greater interaction energies (i.e., had more polarized π systems) would have crystal packing in which the monomers were more closely oriented in a head-to-tail manner. As a consequence of this presumed tight head-to-tail packing, we anticipated that the rate of formation of and the selectivity for the htt *r-ctt* dimers would be greater for those proceeding from a more polar starting material. This hypothesis, however, failed to predict the outcomes of the solid-state irradiation of six azastilbenes. While these results can be rationalized from the crystal structures of the starting materials, the unexpected crystal packing of **15** and **16** highlights the unpredictability associated with rational crystal engineering and the limits that this unpredictability places on the use of solid-state photochemistry to produce synthetically useful products with good control over stereo- and regioselectivity. Indeed, there has been great interest in this field recently, and significant advances have been made in the use of intermolecular templating agents to increase photoreactivity and selectivity in the solid state.⁵³ These include the use of hydrogen-bonding, metal–lone pair interactions, halogen-bonding, and encapsulation approaches.^{54,55} There has been less work in the direct design of molecules that in and of themselves pack in a specific and reactive manner. While examples exist of hydrogen-bonding-enforced diastereoselective solid-state photochemical reactions,⁵⁶ the majority of these examples have focused on engineering a push–pull system in which one arene ring of the diarylethylene system preferentially interacts with the oppositely polarized ring or alkene.^{21,22,57,58} Undoubtedly, this “neat” approach to crystal engineering involving designed hydrogen-bonding or π – π interactions, in which no secondary organizing agent is required, is more efficient. Unfortunately, as described here, efforts to design crystals in this manner can be frustratingly unfruitful, and it may prove that templating techniques are more versatile in their application and hence more useful.⁵⁹ For recent overviews of crystal engineering and [2 + 2] photocycloadditions see the reviews by Natarajan, Biradha, and Elacqua.^{18,54,55}

To our knowledge, this is the first attempt to correlate photoreactivity in the solid state with calculated π system to π system interaction energies. Similar comparisons of irradiation results and the polarity of extended π systems have been made, but only in a generalized fashion.^{24,33,60} Our work in this area was only partially successful, largely due to the unexpected crystal packing of **15** and **16**. If these compounds are excluded from the analysis shown in Figure 5, the hypothesized relationship between binding energy and the percent composition of the *htt r-ctt* dimer in the reaction mixture and the inverse relationship between interaction energy and $t_{1/2}$ become apparent. Indeed, as molecular orientation inside the crystal controls the outcome of irradiation for crystalline solids and prediction of crystal packing remains an unmastered problem, it seems unlikely that the stereoselective synthesis of cyclobutane derivatives through this approach will remain little more than a hit-and-miss situation for the foreseeable future.

Unlike the solid-state irradiations, the solution reactions show a consistent exponential relationship between the percent composition of the *htt r-ctt* dimer in the photolysis mixture and binding energy of the azastilbenes (Figure 10). Of special note is the observation that the cyclobutane formed preferentially from azastilbene **16**, which has the highest calculated *htt* interaction energy of the six irradiated compounds, switches from the *hth r-ctt* dimer formed in the solid state to the anticipated *htt r-ctt* dimer in solution. The excellent correlation observed for selective solution-state formation of the *htt r-ctt* dimer and binding energy suggests that designing stilbene-type compounds that exhibit sufficiently large computational binding energies may be a generally applicable method for attaining solution [2 + 2] photocycloadditions that proceed in synthetically useful regio- and stereochemical yields. Further experimental work would do much to confirm the generality of solution reactivity on the basis of interaction energies.

CONCLUSION

Here, we reported the discovery of a solid-state topochemically controlled [2 + 2] photocycloaddition between two molecules of *trans*-2,4-dichloro-6-styrylpyrimidine (**1**) to form in quantitative yield the associated *htt r-ctt* cyclobutane dimer. Through solution irradiations, 8 of the 10 possible cyclobutane isomers formed from the dimerization of **1** were isolated and identified. The spectral assignments from this analysis were applied to the solid- and solution-state photochemical reactions of **1** and five other azastilbene derivatives (compounds **12–16**) that contained varying degrees of polarization across their extended π systems. Interaction energies between two azastilbene monomers were calculated for each compound using DFT and correlated *ab initio* calculations. While it proved difficult to predict the preferential formation of the *htt r-ctt* dimer in the solid state on the basis of these calculations, due to unpredictable crystal packing of two of the azastilbenes (**15** and **16**), there was a strong correlation between binding energies and *htt r-ctt* cyclobutane formation for all starting materials in solution. It is proposed that the calculation of interaction energies may be a good general tool for the prediction of successful stereo- and regioselective photocycloaddition in solution for stilbene-type compounds.

EXPERIMENTAL SECTION

General Synthetic Methods. All reagents were used as purchased. THF, ether, CH_2Cl_2 , and DMF used in reactions were dried using a solvent delivery system (neutral alumina column).⁶¹ All

reactions were run under a dry N_2 atmosphere except where noted. Flash column chromatography⁶² was performed on flash silica gel (40–64 μM , 60 Å) or using an MPLC system equipped with silica gel columns. ^1H NMR, ^{13}C NMR, and NOE spectra were obtained on 500 MHz FT-NMR spectrometers. Except where noted, both low- and high-resolution mass spectra were obtained using electrospray ionization.

***trans*-2,4-Dichloro-6-styrylpyrimidine (1).** On the basis of the coupling described by Tan et al.⁶³ *trans*-2-phenylvinylboronic acid (2.546 g, 17.2 mmol), K_3PO_4 (7.307 g, 34.4 mmol), and $\text{PdCl}_2(\text{PPh}_3)_2$ (0.362 g, 0.52 mmol) were dissolved in 100 mL of THF. To this mixture was added 2,4,6-trichloropyrimidine (3.156 g, 17.2 mmol) dissolved in 20 mL of THF, producing a cloudy yellow suspension. H_2O (15 mL) was added, and the now clear solution was heated at reflux for 7 h. Approximately 100 mL of H_2O was added, and the biphasic mixture was extracted three times with ether. The combined organic layers were washed with brine and dried over anhydrous MgSO_4 , and the solvent was removed with a rotary evaporator. The product was purified by column chromatography (5–10% EtOAc in hexanes) to provide **1** (3.161 g, 73%). ^1H NMR (500 MHz, CDCl_3): δ 6.95 (d, J = 15.87 Hz, 1 H), 7.22 (s, 1 H), 7.41 (m, 3 H), 7.59 (dd, J = 7.45, 2.08 Hz, 2 H), 7.96 (d, J = 15.87 Hz, 1 H). ^{13}C NMR (500 MHz, CDCl_3): δ 117.1, 123.0, 128.2, 129.2, 130.6, 134.8, 140.9, 160.7, 162.8, 166.6. HRMS (ESI+): m/z calcd for $\text{C}_{12}\text{H}_9\text{N}_2\text{Cl}_2^+$ 251.0143, found 251.0101. Mp: 119–121 °C (recrystallized from EtOAc/hex).

Solution Irradiations of *trans*-2,4-Dichloro-6-styrylpyrimidine (1) in Benzene, Acetonitrile, and Methanol. Solutions of 750 mg (2.98 mmol) of **1** were prepared in 150 mL of benzene, acetonitrile, and methanol. The resulting solution was placed in a photochemical reaction assembly consisting of a water-cooled borosilicate immersion well and surrounding photochemical reactor and was subsequently degassed with vigorous bubbling of N_2 gas for 1.5 h. Irradiation was performed using a 450 W medium-pressure mercury arc lamp for 4–5 h, with mixing of the solution accomplished by continuous bubbling of N_2 through the reaction mixture.

***cis*-2,4-Dichloro-6-styrylpyrimidine (cis-1).** Isolated from solution irradiations of **1** in benzene, acetonitrile, and methanol. ^1H NMR (500 MHz, CDCl_3): δ 6.49 (d, J = 12.22 Hz, 1 H), 7.01 (s, 1 H), 7.15 (d, J = 12.43 Hz, 1 H), 7.27–7.33 (m, 2 H), 7.33–7.38 (m, 3 H). ^{13}C NMR (500 MHz, CDCl_3): δ 118.7, 126.2, 128.6, 128.7, 129.1, 134.8, 140.6, 160.6, 161.8, 167.3. HRMS (ESI+): m/z calcd for $\text{C}_{12}\text{H}_9\text{N}_2\text{Cl}_2^+$ 251.0143, found 251.0140. Mp: 47–48 °C (recrystallized from hexanes).

Isolation of 1,3-Bis(2,4-dichloropyrimid-6-yl)-2,4-diphenylcyclobutanes 2–5 and 7–10. The reaction mixtures from the preceding solution-state irradiations of **1** were combined, and separation of the photoproducts was accomplished by multiple rounds of flash column chromatography using EtOAc/hexanes. Additional separations involving preparative thin-layer chromatography were necessary to isolate some of the lower-yielding photoproducts (developed with EtOAc/hexanes or $\text{CH}_2\text{Cl}_2/\text{EtOAc}$).

r-1,t-3-Bis(2,4-dichloropyrimid-6-yl)-c-2,t-4-diphenylcyclobutane (2; htt r-ctt Isomer). ^1H NMR (500 MHz, CDCl_3): δ 4.64 (dd, J = 10.30, 7.30 Hz, 2 H), 4.84 (dd, J = 10.25, 7.32 Hz, 2 H), 6.93 (s, 2 H), 7.15–7.19 (m, 6 H), 7.25 (d, J = 7.50 Hz, 4 H). ^{13}C NMR (500 MHz, CDCl_3): δ 44.9, 47.3, 119.2, 127.2, 127.5, 128.4, 137.1, 160.1, 161.8, 172.7. HRMS (ESI+): m/z calcd for $\text{C}_{24}\text{H}_{17}\text{N}_4\text{Cl}_4^+$ 501.0207, found 501.0211.

r-1,c-3-Bis(2,4-dichloropyrimid-6-yl)-c-2,t-4-diphenylcyclobutane (3; hth r-cct Isomer). ^1H NMR (500 MHz, CDCl_3): δ 4.36 (t, J = 10.13 Hz, 2 H), 4.63 (t, J = 9.64 Hz, 1 H), 5.22 (t, J = 10.74 Hz, 1 H), 6.92 (d, J = 6.84 Hz, 2 H), 6.97 (s, 2 H), 7.02–7.10 (m, 3 H), 7.32 (t, J = 7.08 Hz, 1 H), 7.40 (t, J = 7.32 Hz, 2 H), 7.44 (d, J = 7.08 Hz, 2 H). ^{13}C NMR (500 MHz, CDCl_3): δ 42.9, 48.5, 48.8, 118.6, 121.6, 126.7, 127.43, 127.45, 128.36, 128.9, 129.3, 134.7, 160.3, 162.0, 172.3. HRMS (ESI+): m/z calcd for $\text{C}_{24}\text{H}_{17}\text{N}_4\text{Cl}_4^+$ 501.0207, found 501.0207.

r-1,t-3-Bis(2,4-dichloropyrimid-6-yl)-c-2,c-4-diphenylcyclobutane (4; htt r-ctc Isomer). ^1H NMR (500 MHz, CDCl_3): δ 4.40 (t, J = 8.68 Hz, 1 H), 4.63 (t, J = 9.43 Hz, 2 H), 5.25 (t, J = 10.29 Hz, 1 H), 6.90 (s, 1 H), 7.13 (d, J = 7.29 Hz, 6 H), 7.22 (t, J = 7.93 Hz, 4 H), 7.49 (s,

1 H). ^{13}C NMR (500 MHz, CDCl_3): δ 45.8, 46.7, 50.2, 119.0, 120.8, 126.2, 127.1, 128.3, 136.8, 159.2, 161.2, 162.0, 162.8, 172.0, 173.8. HRMS (ESI+): m/z calcd for $\text{C}_{24}\text{H}_{17}\text{N}_4\text{Cl}_4^+$ 501.0207, found 501.0220.

r-1,c-3-Bis(2,4-dichloropyrimid-6-yl)-t-2,t-4-diphenylcyclobutane (5; htt r-ctt Isomer). ^1H NMR (500 MHz, CDCl_3): δ 3.78 (t, $J = 9.54$ Hz, 2 H), 4.20 (t, $J = 9.65$ Hz, 2 H), 7.14 (s, 2 H), 7.27 (d, $J = 6.86$ Hz, 4 H), 7.31 (d, $J = 7.29$ Hz, 2 H), 7.37 (t, $J = 7.90$ Hz, 4 H). ^{13}C NMR (500 MHz, CDCl_3): δ 47.7, 52.1, 118.5, 124.9, 126.8, 127.7, 129.0, 139.7, 162.6, 173.2. HRMS (ESI+): m/z calcd for $\text{C}_{24}\text{H}_{17}\text{N}_4\text{Cl}_4^+$ 501.0207, found 501.0202.

r-1,c-2-Bis(2,4-dichloropyrimid-6-yl)-t-3,t-4-diphenylcyclobutane (7; hth r-ctt Isomer). ^1H NMR (500 MHz, CDCl_3): δ 3.97 (AA'BB', 2 H), 4.09 (AA'BB', 2 H), 7.13 (s, 2 H), 7.30 (d, $J = 7.07$ Hz, 6 H), 7.37 (t, $J = 7.07$ Hz, 4 H). ^{13}C NMR (500 MHz, CDCl_3): δ 49.2, 50.2, 118.8, 127.0, 127.6, 128.9, 140.2, 161.1, 162.6, 172.7. HRMS (ESI+): m/z calcd for $\text{C}_{24}\text{H}_{17}\text{N}_4\text{Cl}_4^+$ 501.0207, found 501.0201.

r-1,t-2-Bis(2,4-dichloropyrimid-6-yl)-c-3,c-4-diphenylcyclobutane (8; hth r-ctt Isomer). ^1H NMR (500 MHz, CDCl_3): δ 4.27–4.33 (q, $J = 8.55$ Hz, 2 H), 4.49 (t, $J = 8.79$ Hz, 1 H), 5.13 (t, $J = 10.74$ Hz, 1 H), 6.87 (s, 1 H), 7.13 (t, $J = 8.06$ Hz, 4 H), 7.21 (t, $J = 7.57$ Hz, 2 H), 7.37 (d, $J = 4.15$ Hz, 4 H), 7.44 (s, 1 H). HRMS (ESI+): m/z calcd for $\text{C}_{24}\text{H}_{17}\text{N}_4\text{Cl}_4^+$ 501.0207, found 501.0208.

r-1,c-2-Bis(2,4-dichloropyrimid-6-yl)-t-3,c-4-diphenylcyclobutane (9; hth r-ctt Isomer). ^1H NMR (500 MHz, CDCl_3): δ 4.57 (quin, $J = 9.46$ Hz, 2 H), 4.76 (t, $J = 9.77$ Hz, 1 H), 4.97 (dd, $J = 10.62, 8.91$ Hz, 1 H), 6.79 (d, $J = 0.49$ Hz, 1 H), 6.83 (dd, $J = 7.57, 1.71$ Hz, 2 H), 6.95 (d, $J = 8.06$ Hz, 2 H), 6.98–7.03 (m, 3 H), 7.08 (t, $J = 7.08$ Hz, 1 H), 7.15 (t, $J = 7.57$ Hz, 2 H), 7.57 (s, 1 H). HRMS (ESI+): m/z calcd for $\text{C}_{24}\text{H}_{17}\text{N}_4\text{Cl}_4^+$ 501.0207, found 501.0195.

r-1,t-2-Bis(2,4-dichloropyrimid-6-yl)-c-3,t-4-diphenylcyclobutane (10; hth r-ctt Isomer). ^1H NMR (500 MHz, CDCl_3): δ 3.95–3.98 (AA'BB' q, 2 H) 4.07–4.11 (AA'BB' q, 2 H) 7.12 (s, 2 H) 7.28–7.32 (m, 6 H) 7.35–7.39 (m, 4 H). ^{13}C NMR (500 MHz, CDCl_3): δ 46.4, 47.0, 119.4, 126.8, 127.7, 128.4, 137.9, 160.2, 162.8, 173.0. HRMS (ESI+): m/z calcd for $\text{C}_{24}\text{H}_{17}\text{N}_4\text{Cl}_4^+$ 501.0207, found 501.0200.

trans-2,4-Dimethoxy-6-styrylpyrimidine (12). A 0.500 g portion (1.99 mmol) of *trans*-2,4-dichloro-6-styrylpyrimidine (**1**) was dissolved in 10 mL of 25%, by weight, NaOMe/MeOH. The resulting solution was heated at reflux for 12 h. After being cooled to room temperature, the reaction mixture was extracted from water three times with Et_2O . The combined organic layers were washed with saturated NaCl solution and dried over anhydrous MgSO_4 , and the solvent was removed with a rotary evaporator. The crude solid was recrystallized from EtOAc/hexanes to give 0.174 g (0.72 mmol, 36% yield) of pure **12**. ^1H NMR (500 MHz, CDCl_3): δ 4.00 (s, 3 H), 4.07 (s, 3 H), 6.35 (s, 1 H), 6.95 (d, $J = 15.63$ Hz, 1 H), 7.34 (t, $J = 7.57$ Hz, 1 H), 7.39 (t, $J = 7.32$ Hz, 2 H), 7.59 (d, $J = 7.32$ Hz, 2 H), 7.87 (d, $J = 15.87$ Hz, 1 H). ^{13}C NMR (500 MHz, CDCl_3): δ 53.7, 54.6, 99.5, 125.5, 127.4, 128.7, 128.9, 135.8, 136.1, 164.0, 165.1, 172.3. HRMS (ESI+): m/z calcd for $\text{C}_{14}\text{H}_{15}\text{N}_2\text{O}_2^+$ 243.1134, found 243.1127. Mp: 47–48 °C (recrystallized from EtOAc/hexanes).

trans-4-Styrylpyrimidine (13). A 0.400 g portion (3.5 mmol) of 4-chloropyrimidine, 0.516 g (3.5 mmol) of *trans*-2-phenylvinylboronic acid, 0.074 g (0.105 mmol) of $\text{Pd}(\text{Cl}_2)(\text{PPh}_3)_2$, and 2.23 g (10.5 mmol) of K_3PO_4 were combined in 26 mL of THF. To this heterogeneous mixture was added 3.24 mL of H_2O . The resulting solution was heated to reflux overnight. The reaction mixture was cooled to room temperature, and approximately 50 mL of water was added. The resulting biphasic mixture was extracted three times with ether. The combined organic layers were washed with brine and dried over anhydrous MgSO_4 , and the solvent was removed with a rotary evaporator. The product was purified by column chromatography (25% EtOAc in hexanes) to provide pure **13** (0.442 g, 70% yield). ^1H NMR (500 MHz, CDCl_3): δ 7.02 (d, $J = 15.87$ Hz, 1 H), 7.26 (d, $J = 5.15$ Hz, 1 H), 7.30–7.41 (m, 3 H), 7.56 (d, $J = 7.07$ Hz, 2 H), 7.86 (d, $J = 15.86$ Hz, 1 H), 8.63 (d, $J = 5.15$ Hz, 1 H), 9.15 (s, 1 H). ^{13}C NMR (500 MHz, CDCl_3): δ 118.4, 125.5, 127.6, 128.7, 129.3, 135.5, 137.4, 157.2, 158.8, 162.1. HRMS (ESI+): m/z calcd for $\text{C}_{12}\text{H}_{11}\text{N}_2^+$

183.0922, found 183.0919. Mp: 70–71 °C (recrystallized from EtOAc/hexanes).

trans-2,4-Dichloro-6-styrylpyridine (14). A 0.500 g portion (2.74 mmol) of 2,4,6-trichloropyridine, 0.487 g (3.29 mmol) of *trans*-2-phenylvinylboronic acid, 0.057 g (0.082 mmol) of $\text{Pd}(\text{Cl}_2)(\text{PPh}_3)_2$, and 1.17 g (5.48 mmol) of K_3PO_4 were combined in 20 mL of THF. To this heterogeneous mixture was added 2.5 mL of H_2O . The resulting solution was heated to reflux for 20 h. After being cooled to room temperature, the resulting residue was extracted from water three times with ether. The combined organic layers were washed with brine and dried over anhydrous MgSO_4 , and the solvent was removed with a rotary evaporator. The product was purified by column chromatography (5–10% EtOAc in hexanes) to provide pure **14** (0.323 g, 47% yield). ^1H NMR (500 MHz, CDCl_3): δ 7.01 (d, $J = 16.08$ Hz, 1 H), 7.19 (s, 1 H), 7.25 (s, 1 H), 7.34 (t, $J = 7.07$ Hz, 1 H), 7.40 (t, $J = 7.50$ Hz, 2 H), 7.57 (d, $J = 7.29$ Hz, 2 H), 7.70 (d, $J = 15.87$ Hz, 1 H). ^{13}C NMR (500 MHz, CDCl_3): δ 120.6, 121.9, 125.1, 127.4, 128.8, 129.0, 135.6, 135.7, 145.8, 151.7, 157.1. HRMS (ESI+): m/z calcd for $\text{C}_{13}\text{H}_{10}\text{NCl}_2^+$ 250.0190, found 250.0188. Mp: 36–38 °C (recrystallized from EtOAc/hexanes).

trans-2,4-Dichloro-6-(2-(pyridin-2-yl)vinyl)pyrimidine (15). A 27 mg portion of NaH (0.67 mmol, 60% dispersion in mineral oil) was added to 4 mL of THF. To this suspension was added 2,4-dichloro-6-methylpyrimidine (0.100 g, 0.61 mmol) dissolved in 2 mL of THF. The resulting cloudy yellow solution was stirred for 10 min at room temperature, after which 140 μL (1.23 mmol) of 2-pyridylcarboxaldehyde was added dropwise. Upon complete addition of the aldehyde, the reaction mixture turned from a cloudy yellow to a clear orange. The reaction was stirred at room temperature for 30 min, quenched with H_2O , and extracted three times with ether. The combined organic layers were washed with saturated NaCl solution and dried over anhydrous magnesium sulfate. After removal of solvent by a rotary evaporator, the resulting residue was purified by MPLC on a silica gel column using a 0–50% 1% TEA in EtOAc/hexanes gradient elution to provide 46 mg (0.18 mmol, 30% yield) of **15**. ^1H NMR (500 MHz, CDCl_3): δ 7.26 (s, 1 H), 7.29 (ddd, $J = 7.56, 4.77, 1.18$ Hz, 1 H), 7.46 (d, $J = 7.72$ Hz, 1 H), 7.56 (d, $J = 15.44$ Hz, 1 H), 7.75 (td, $J = 7.66, 1.82$ Hz, 1 H), 8.00 (d, $J = 15.22$ Hz, 1 H), 8.67 (d, $J = 3.65$ Hz, 1 H). ^{13}C NMR (500 MHz, CDCl_3): δ 118.2, 124.2, 125.1, 126.7, 137.0, 139.0, 150.2, 152.9, 160.6, 163.0, 165.9. HRMS (ESI+): m/z calcd for $\text{C}_{11}\text{H}_8\text{N}_3\text{Cl}_2^+$ 252.0095, found 252.0095. Mp: 153–154 °C (recrystallized from EtOAc/hexanes).

trans-2,4-Dichloro-6-(4-methoxystyryl)pyrimidine (16). A 108 mg portion of NaH (2.70 mmol, 60% dispersion in mineral oil) was added to 8 mL of THF. To this suspension was added 2,4-dichloro-6-methylpyrimidine (0.200 g, 1.22 mmol) dissolved in 4 mL of THF. The resulting cloudy yellow solution was stirred for 5 min at room temperature, after which 150 μL (1.23 mmol) of 4-methoxybenzaldehyde was added dropwise. The reaction mixture was stirred at room temperature under a constant weak stream of nitrogen, with the N_2 efflux passing directly from the flask through a needle fitted with a Drierite drying tube. Under these conditions, the solvent was allowed to slowly evaporate, leaving behind a reddish orange solid. The residue was dissolved in CH_2Cl_2 and extracted from water three times. The combined organic layers were washed with saturated NaCl solution and dried over anhydrous magnesium sulfate. After removal of solvent by rotary evaporation, the resulting residue was purified by MPLC on a silica gel column using a 35–100% CH_2Cl_2 /hexanes gradient elution to provide 54 mg (0.19 mmol, 15% yield) of **16**. ^1H NMR (500 MHz, CDCl_3): δ 3.86 (s, 3 H), 6.81 (d, $J = 15.65$ Hz, 1 H), 6.94 (d, $J = 8.79$ Hz, 2 H), 7.18 (s, 1 H), 7.55 (d, $J = 8.79$ Hz, 2 H), 7.92 (d, $J = 15.86$ Hz, 1 H). ^{13}C NMR (500 MHz, CDCl_3): δ 55.4, 114.5, 116.4, 120.5, 127.5, 129.8, 140.5, 160.4, 161.5, 162.3, 166.8. HRMS (ESI+): m/z calcd for $\text{C}_{13}\text{H}_{11}\text{N}_2\text{OCl}_2^+$ 281.0248, found 281.0249. Mp: 127–128 °C (recrystallized from EtOAc/hexanes).

Solid-State Irradiations/Rate Studies. Irradiations were accomplished using a 68 W compact fluorescent light bulb (300 W incandescent equivalent, 2700 K color temperature) placed in a 0.5 m³ box that was completely encased in aluminum foil. With this setup the

air temperature in the irradiation box did not rise above 30 °C, and the temperature on the water-cooled plate was a constant 23–25 °C. Prior to irradiation of each sample, the bulb was allowed to warm up for at least 30 min. For each irradiation 45–50 mg of azastilbene (compounds **1** and **12–16**, each recrystallized from EtOAc/hexanes) was ground to a fine powder using a mortar and pestle. The powder was then spread evenly on a water-cooled borosilicate glass plate over an area of approximately 9 × 9 cm. The sample was then covered with a borosilicate glass plate, which was firmly pressed into place to further ensure an even distribution of the solid. The samples were placed approximately 7–8 cm beneath the 68 W bulb and irradiated for times ranging from 2 to 24 h, depending on the rate of photocycloaddition. Time points were taken every 10 min for the first 2 h and generally every 30–60 min thereafter. Time-point samples were obtained using a microspatula after brisk removal of the cover slide, and efforts were made to ensure that these samples were representative of a broad area of the irradiated solid. The crude irradiation samples were dissolved in CDCl₃, and analyzed for relative integration of proton signals using a 500 MHz narrow-bore spectrometer.

Solution-State Irradiations/Rate Studies. The same irradiation setup used for the solid-state rate studies was used for the solution-state rate studies, with the exception that the samples were not water-cooled. For each sample, 40 mM solutions of each azastilbene (compounds **2** and **12–16**) in CDCl₃ were placed in sealed borosilicate NMR tubes. The samples were irradiated simultaneously for 24 h, removed from the light source, and directly analyzed by ¹H NMR using a 500 MHz narrow-bore spectrometer. Evaporated solvent was replaced, and the samples were irradiated for an additional 24 h. This was repeated five times for a total of 120 h of irradiation.

Data Analysis. Data analysis for the solid-state reactions was accomplished using Graphpad Prism 5.0, fitted to a first-order exponential decay curve. Data analysis for solution-state reactions was performed using OriginPro 8.5, with data fitted to an exponential least-squares fit curve.

Crystallography. Cyclobutane **2** was recrystallized from MeOH. The azastilbenes **1**, *cis*-**1**, and **16** were recrystallized from EtOAc/hexanes. Crystal and structure refinement data can be found in the Supporting Information.

■ ASSOCIATED CONTENT

● Supporting Information

Figures, tables, text, and CIF files giving additional ¹H NMR spectra, photolysis reaction curves, X-ray crystal structure refinement data for **1**, *cis*-**1**, **2**, and **16**, computational details, xyz coordinates, and absolute energies. This material is available free of charge via the Internet at <http://pubs.acs.org>.

■ AUTHOR INFORMATION

Corresponding Author

*J.A.K.: tel, 217 333 6310; e-mail, jkatzene@illinois.edu.

Notes

The authors declare no competing financial interest.

■ ACKNOWLEDGMENTS

X-ray crystal structures were obtained at the George L. Clark X-ray facility at the University of Illinois at Urbana-Champaign. We thank Brigham Young University and the Fulton Supercomputing Laboratory for computational resources. We are grateful for support of this research from a grant from the U.S. Army Medical Research Command (W81WXH-10-1-0179, to J.A.K.) and a fellowship from the National Institutes of Health (NRSA 1 F30 DK083899, to A.A.P.).

■ REFERENCES

(1) Liebermann, C.; Bergami, O. *Ber. Dtsch. Chem. Ges.* **1889**, *22*, 782.

(2) Marckwald, W. Z. *Phys. Chem., Stoichiomet. Verwandtschaftsftl.* **1899**, *30*, 140.

(3) Ciamician, G.; Silber, P. *Ber. Dtsch. Chem. Ges.* **1901**, *34*, 2040.

(4) Senier, A.; Shephard, F. G. *J. Chem. Soc., Trans.* **1909**, *95*, 1943.

(5) Kohlschutter, V.; Haenni, P. Z. *Anorg. Allg. Chem.* **1919**, *105*, 121.

(6) Stobbe, H.; Steinberger, F. K. *Ber. Dtsch. Chem. Ges. B* **1922**, *55B*, 2225.

(7) Bernstein, H. I.; Quimby, W. C. *J. Am. Chem. Soc.* **1943**, *65*, 1845.

(8) Schmidt, G. M. J. *J. Pure Appl. Chem.* **1971**, *27*, 647.

(9) Cohen, M. D.; Schmidt, G. M. J. *J. Chem. Soc.* **1964**, 1996.

(10) Cohen, M. D.; Schmidt, G. M. J.; Sonntag, F. I. *J. Chem. Soc.* **1964**, 2000.

(11) Schmidt, G. M. J. *J. Chem. Soc.* **1964**, 2014.

(12) Cohen, M. D. *Angew. Chem.* **1975**, *87*, 439.

(13) Gnanaguru, K.; Ramasubbu, N.; Venkatesan, K.; Ramamurthy, V. *J. Org. Chem.* **1985**, *50*, 2337.

(14) Bhadbhade, M. M.; Murthy, G. S.; Venkatesan, K.; Ramamurthy, V. *Chem. Phys. Lett.* **1984**, *109*, 259.

(15) Murthy, G. S.; Arjunan, P.; Venkatesan, K.; Ramamurthy, V. *Tetrahedron* **1987**, *43*, 1225.

(16) Ramdas, S.; Jones, W.; Thomas, J. M.; Desvergne, J. P. *Chem. Phys. Lett.* **1978**, *57*, 468.

(17) Natarajan, A.; Ramamurthy, V. *Chem. Cyclobutanes* **2005**, *2*, 807.

(18) Natarajan, A.; Bhogala, B. R. *Supramol. Photochem.* **2011**, 175.

(19) Ito, Y.; Kajita, T.; Kunimoto, K.; Matsuura, T. *J. Org. Chem.* **1989**, *54*, 587.

(20) Syamala, M. S.; Ramamurthy, V. *J. Org. Chem.* **1986**, *51*, 3712.

(21) Papagni, A.; Del Buttero, P.; Bertarelli, C.; Miozzo, L.; Moret, M.; Pryce, M. T.; Rizzato, S. *New J. Chem.* **2010**, *34*, 2612.

(22) Coates, G. W.; Dunn, A. R.; Henling, L. M.; Ziller, J. W.; Lobkovsky, E. B.; Grubbs, R. H. *J. Am. Chem. Soc.* **1998**, *120*, 3641.

(23) Stegemeyer, H. *Chimia* **1965**, *19*, 536.

(24) Ulrich, H.; Rao, D. V.; Stuber, F. A.; Sayigh, A. A. R. *J. Org. Chem.* **1970**, *35*, 1121.

(25) Williams, J. L. R.; Webster, S. K.; Van Allan, J. A. *J. Org. Chem.* **1961**, *26*, 4893.

(26) Williams, J. L. R. *J. Org. Chem.* **1960**, *25*, 1839.

(27) Williams, J. L. R.; Carlson, J. M.; Reynolds, G. A.; Adel, R. E. *J. Org. Chem.* **1963**, *28*, 1317.

(28) Horner, M.; Huenig, S. *Liebigs Ann. Chem.* **1982**, 1183.

(29) Yamada, S.; Uematsu, N.; Yamashita, K. *J. Am. Chem. Soc.* **2007**, *129*, 12100.

(30) Vansant, J.; Toppet, S.; Smets, G.; Declercq, J. P.; Germain, G.; Van Meerssche, M. *J. Org. Chem.* **1980**, *45*, 1565.

(31) Mondal, B.; Captain, B.; Ramamurthy, V. *Photochem. Photobiol. Sci.* **2011**, *10*, 891.

(32) Chung, C.; Nakamura, F.; Hashimoto, Y.; Hasegawa, M. *Chem. Lett.* **1991**, 779.

(33) Kaupp, G.; Frey, H.; Behmann, G. *Chem. Ber.* **1988**, *121*, 2135.

(34) Kato, T.; Katagiri, N.; Takahashi, T.; Katagiri, Y. *J. Heterocycl. Chem.* **1979**, *16*, 1575.

(35) Hasegawa, M.; Endo, Y.; Aoyama, M.; Saigo, K. *Bull. Chem. Soc. Jpn.* **1989**, *62*, 1556.

(36) *Pure Appl. Chem.* **1976**, *45*, 11.

(37) Whitten, D. G.; Lee, Y. J. *J. Am. Chem. Soc.* **1972**, *94*, 9142.

(38) Dudek, R. C.; Anderson, N. T.; Donnelly, J. M. *Chem. Educ.* **2011**, *16*, 76.

(39) Vaske, Y. S. M.; Mahoney, M. E.; Konopelski, J. P.; Rogow, D. L.; McDonald, W. J. *J. Am. Chem. Soc.* **2010**, *132*, 11379.

(40) Wheeler, S. E.; Houk, K. N. *J. Am. Chem. Soc.* **2008**, *130*, 10854.

(41) Wheeler, S. E.; Houk, K. N. *J. Chem. Theory Comput.* **2009**, *9*, 2301.

(42) Frisch, M. J.; Trucks, G. W.; Schlegel, H. B.; Scuseria, G. E.; Robb, M. A.; Cheeseman, J. R.; Scalmani, G.; Barone, V.; Mennucci, B.; Petersson, G. A.; Nakatsuji, H.; Caricato, M.; Li, X.; Hratchian, H. P.; Izmaylov, A. F.; Bloino, J.; Zheng, G.; Sonnenberg, J. L.; Hada, M.; Ehara, M.; Toyota, K.; Fukuda, R.; Hasegawa, J.; Ishida, M.; Nakajima, T.; Honda, Y.; Kitao, O.; Nakai, H.; Vreven, T.; Montgomery, Jr., J. A.; Peralta, J. E.; Ogliaro, F.; Bearpark, M.; Heyd, J. J.; Brothers, E.; Kudin,

K. N.; Staroverov, V. N.; Kobayashi, R.; Normand, J.; Raghavachari, K.; Rendell, A.; Burant, J. C.; Iyengar, S. S.; Tomasi, J.; Cossi, M.; Rega, N.; Millam, N. J.; Klene, M.; Knox, J. E.; Cross, J. B.; Bakken, V.; Adamo, C.; Jaramillo, J.; Gomperts, R.; Stratmann, R. E.; Yazyev, O.; Austin, A. J.; Cammi, R.; Pomelli, C.; Ochterski, J. W.; Martin, R. L.; Morokuma, K.; Zakrzewski, V. G.; Voth, G. A.; Salvador, P.; Dannenberg, J. J.; Dapprich, S.; Daniels, A. D.; Farkas, Ö.; Foresman, J. B.; Ortiz, J. V.; Cioslowski, J.; Fox, D. J. *Gaussian 09*; Gaussian, Inc., Wallingford, CT, 2009.

- (43) Zhao, Y.; Truhlar, D. G. *Acc. Chem. Res.* **2008**, *41*, 157.
(44) Grimme, S. *J. Chem. Phys.* **2003**, *118*, 9095.
(45) Loader, C. E.; Timmons, C. J. *J. Chem. Soc.* **1967**, 1343.
(46) Hazai, L.; Hornyak, G. *ACH - Models Chem.* **1998**, *135*, 493.
(47) Perkampus, H. H.; Bluhm, T. *Tetrahedron* **1972**, *28*, 2099.
(48) Fehn, H.; Perkampus, H. H. *Tetrahedron* **1978**, *34*, 1971.
(49) Leiserowitz, L.; Schmidt, G. M. J. *Acta Crystallogr.* **1965**, *18*, 1058.
(50) Steiner, T. *NATO Sci. Ser., Ser. E* **1999**, *360*, 185.
(51) Desiraju, G. R. *Acc. Chem. Res.* **2002**, *35*, 565.
(52) Desiraju, G. R. *J. Am. Chem. Soc.* **2013**, *135*, 9952.
(53) Nagarathinam, M.; Peedikakkal, A. M. P.; Vittal, J. J. *Chem. Commun.* **2008**, 5277.
(54) Biradha, K.; Santra, R. *Chem. Soc. Rev.* **2013**, *42*, 950.
(55) Elacqua, E.; Laird, R. C.; MacGillivray, L. R. *Supramol. Chem.: Mol. Nanomater.* **2012**, *6*, 3153.
(56) Feldman, K. S.; Campbell, R. F. *J. Org. Chem.* **1995**, *60*, 1924.
(57) Marras, G.; Metrangolo, P.; Meyer, F.; Pilati, T.; Resnati, G.; Vij, A. *New J. Chem.* **2006**, *30*, 1397.
(58) Liu, J.; Wendt, N. L.; Boarman, K. J. *Org. Lett.* **2005**, *7*, 1007.
(59) Bhogala, B. R.; Captain, B.; Parthasarathy, A.; Ramamurthy, V. J. *Am. Chem. Soc.* **2010**, *132*, 13434.
(60) Song, Q.-H.; Wang, H.-B.; Li, X.-B.; Hei, X.-M.; Guo, Q.-X.; Yu, S.-Q. *J. Photochem. Photobiol., A* **2006**, *183*, 198.
(61) Pangborn, A. B.; Giardello, M. A.; Grubbs, R. H.; Rosen, R. K.; Timmers, F. J. *Organometallics* **1996**, *15*, 1518.
(62) Still, W. C.; Kahn, M.; Mitra, A. J. *Org. Chem.* **1978**, *43*, 2923.
(63) Tan, J.; Chang, J.; Deng, M. *Synth. Commun.* **2004**, *34*, 3773.